糖尿病マウス病理所見(CD34 免疫染色 day4)

CD34 immunohistochemical method in each group on day 4 after initial wounding.

図3

[IV]

研究成果の刊行に関する一覧表

Nanba D, Inoue H, Shigemi Y, Shirakata Y, Hashimoto K, Higashiyama S: An intermediary role of proHB-EGF shedding in growth factor-induced c-Myc gene expression. J Cell Physiol 214:465-73, 2008

Dai X, Sayama K, Shirakata Y, Tokumaru S, Yang L, Tohyama M, Hirakawa S, Hanakawa Y, Hashimoto K: PPARgamma is an important transcription factor in 1alpha, 25-dihydroxyvitamin D3-induced involucrin expression. J Dermatol Sci 50:53-60, 2008

Dai X, Sayama K, Tohyama M, Shirakata Y, Yang L, Hirakawa S, Tokumaru S, Hashimoto K: The NF-kB, p38 MAPK and STAT1 pathways differentially regulate the dsRNA-mediated innate immune responses of epidermal keratinocytes. Int Immunol 20:901-9, 2008

Yura H, Kanatani Y, Ishihara M, Takase B, Nambu M, Kishimoto S, Kitagawa M, Tatsuzawa O, Hoshi Y, Suzuki S, Kawakami M, Matsui T: Selection of hematopoietic stem cells with a combination of galactose-bound vinyl polymer and soybean agglutinin, a galactose-specific lectin. Transfusion 48:561-6, 2008

Nakamura S, Nambu M, Ishizuka T, Hattori H, Kanatani Y, Kishimoto S, Takase B, Aoki H, Kiyosawa T, Maehara T, Ishihara M: Effect of controlled release of fibroblast growth factor-2 from chitosan/fucoidan micro complex-hydrogel on in vitro and in vivo vascularization. J Biomed Mater Res (A) 85:619-27, 2008

Nakamura S, Watanabe S, Ohtsuka M, Maehara T, Ishihara M, Yokomine T, Sato M: Cre-loxP system as a versatile tool for conferring increased levels of tissue-specific gene expression from a weak promoter. Mol Reprod Dev 75:1085-93, 2008

Hattori H, Yashiro N, Tanaka T, Amano Y, Fukuda K, Kishimoto S, Kanatani Y, Nakamura S, Takase B, Ishihara M: Expansion and characterization of adipose tissue-derived stromal cells cultured with low serum medium. J Biomed Mater Res 87:229-36, 2008

Nogami Y, Kinoshita M, Takase B, Ogata Y, Saitoh D, Kikuchi M, Ishihara M, Maehara T: Liposome-encapsulated hemoglobin transfusion rescues rats undergoing progressive hemodilution from lethal organ hypoxia without scavenging nitric oxide. Ann Surg 248:310-319, 2008

Maemura T, Shin T, Kinoshita M, Majima T, Ishihara M, Saitoh D, Ichikura T: A tissue-engineered stomach shows presence of proton pump and G-cells in rat model, resulting in improved anemia following total gastrectomy. Artif Org 32: 234-9, 2008.

Ishizuka T, Ishihara M, Aiko S, Nogami Y, Nakamura S, Kanatani Y, Kishimoto S, Hattori H, Horio T, Tanaka Y, Maehara T: Experimental evaluation of photocrosslinkable chitosan hydrogel as injection solution for endoscopic resection. Endoscopy 41:25-8, 2009

Tsuda Y, Ishihara M, Amako M, Arino H, Hattori H, Kanatani Y, Yura H, NemotoK: Photocrosslinkable chitosan hydrogel can prevent of bone formation in rat skull and fibula bone defects with. Artif Org 33:74-7, 2009

Kishimoto S, Nakamura S, Nakamura S, Hattori H, Oomuma F, Kanatani Y, Tanaka Y, Harada Y, Tagawa M, Maehara T, Ishihara M: Cytokine-immobilized microparticle-coated plates for culturing hematopoietic progenitor cells. J Controlled Release 133:185-90, 2009

Kishimoto S, Nakamura S, Hattori H, Nakamura SI, Oonuma F, Kanatani Y, Tanaka Y, Mori Y, Harada Y, Tagawa M, Ishihara M: Human Stem Cell Factor (SCF) is a Heparin-Binding Cytokine. J Biochem 145:275-278, 2009

Nambu M, Kishimoto S, Nakamura S, Mizuno H, Yanagibayashi S, Yamamoto N, Azuma R, Nakamura S, Kiyosawa T, Ishihara M, Kanatani Y: Accelerated Wound Healing in Healing Impaired *db/db* Mice by Autologous Adipose Tissue-Derived Stromal Cells Combined with Atelocollagen Matrix. Ann Plast Surg 62:317-21, 2009

Yura H, Ishihara M, Nakamura S, Kishimoto S, Kanatani Y, Horio T, Ishizuka T, Kawakami M, Matsui T: Coatings of LDL and synthetic glycoconjugates as substrata for hepatocytes. Artif Org 2009 in press

Nakamura S, Kanatani Y, Kishimoto S, Nakamura S, Ohno C, Horio T, M, Hattori H, Tanaka Y, Kiyosawa T, Maehara T, Ishihara M: Controlled release of FGF-2 using fragmin/protamine microparticles and effect on neovascularization. J Biomed Mater Res (A) 2009 in press

Nakamura S, Kishimoto S, Nakamura S, Nambu M, Fujita M, Tanaka Y, Mori Y, Tagawa M, Maehara T, Ishihara M: Fragmin/protamine microparticles as cell carriers to enhance viability of adipose-derived stromal cells and their subsequent effect on in vivo neovascularization. J Biomed Mater Res (A) 2009 in press

Nakamura S, Ishihara M, Takikawa M, Murakami K, Mishicot S, Nakamura S, Yanagibayashi S, Kubo S, Yamamoto N, Kiyosawa T: Platelet-Rich Plasma (PRP) Promote Survival of Inbred Fat-Graft in Rats. Ann Plast Surg 2009 in press

Satoh Y, Saitoh D, Takeuchi A, Ojima K, Kouzu K, Kawakami S, Ito M, Ishihara M, Shunichi Sato S, Takishima K: ERK2 dependent signaling contributes to wound healing after a partial-thickness burn. Biochem Biophys Res Commun 2009 in press

Horio T, Ishihara M, Fujita M, Kishimoto S, Kanatani Y, Ishizuka T, Nogami Y, Nakamura S, Tanaka Y, Maehara T: Hemostatic Effects of Photocrosslinkable Chitosan Hydrogel-Mixed Photocrosslinked Chitosan Sponges (PCM-S) on Hepatic Bleeding in Rats. Artif Org 2009 in press

Kishimoto S, Oonuma F, Nakamura S, Hattori H, Nakamura S, Mori Y, Tanaka Y, Harada Y, Tagawa M, Ishihara M: Immobilization, Stabilization, and Activation of Human Stem Cell Factor (SCF) on Fragmin/Protamine Microparticle (F/P MP)-Coated Plates. J Biomed Mater Res (B) 2009 in press

Kishimoto S, Hattori H, Nakamura S, Amano Y, Kanatani Y, Tanaka Y, Harada Y, Tagawa M, Ishihara M: Expansion and characterization of human bone marrow-derived mesenchymal stem cells cultured on fragmin/protamine microparticle-coated matrix with FGF-2 in low serum medium. Tissue Eng 2009 in press

Kishimoto S, Nakamura S, Nakamura S, Kanatani Y, Hattori H, Tanaka Y, Harada Y, Tagawa M, Maehara T, Ishihara M: Fragmin/Protamine Microparticle (F/P MP)-Coated Matrix Immobilized Cytokines to Stimulate Various Cell Proliferations with Low serum Media. Artif Org 2009 in press

青木幸一, 木下学, 庄野聡, 野上弥志郎, 高瀬凡平, 石原雅之, 山田憲彦, 菊地眞, 齋藤大蔵. 人工赤血球の骨髄内投与による致死的出血性ショックに対する救命蘇生効果. 防衛衛生　55(2):　p.29-37,　2008.02.

岸本聡子, 中村伸吾, 服部秀美, 石原雅之. 成長因子とヘパラン硫酸プロテオグリカンの相互作用. 生体の科学　59(2):　p.92-100,　2008.04.

片桐彰男, 橋谷華世, 中村伸吾, 服部秀美, 岸本聡子, 前原正明, 石原雅之. FGF-2 含有フラグミンプロタミンマイクロキャリア(F/P MPs)による虚血改善効果の検討. 防衛衛生　56(1):　p.17-24,　2009.01.

山本直人, 中村真一郎, 東隆一, 柳林 聡, 清澤智晴, 山本直人, 中村真一郎, 東隆一, 柳林 聡, 清澤智晴. 脂肪腫摘出術後に生じた Chronic expanding hematoma の 1 例. 日本形成外科学会会誌　28(5):328-335,　2008.

山本直人, 南部正樹, 植田晃史, 千々和剛, 大竹登志江, 小倉奈加, 東隆一, 清澤智晴. 術後予防的抗菌剤の投与期間に関する検討 ー外来での皮膚軟部腫瘍摘出においてー. Skin Surgery　16(3):137-140, 2008.

加藤摩衣, 泉 彰典, 瀧川恵美, 柳林 聡, 南部正樹, 東隆一, 山本直人, 清澤智晴. 鼻尖部腫瘤に対する Midline incision の有用性. Skin Surgery　16(3):122-125, 2008.

[V]

别刷

Journal of Cellular Physiology

An Intermediary Role of proHB-EGF Shedding in Growth Factor-induced *c-Myc* Gene Expression

DAISUKE NANBA,[1] HIROFUMI INOUE,[1] YUKA SHIGEMI,[1] YUJI SHIRAKATA,[2] KOJI HASHIMOTO,[2] AND SHIGEKI HIGASHIYAMA[1,3]*

[1]*Department of Biochemistry and Molecular Genetics, Ehime University Graduate School of Medicine, Shitsukawa, Toon, Ehime, Japan*

[2]*Department of Dermatology, Ehime University Graduate School of Medicine, Shitsukawa, Toon, Ehime, Japan*

[3]*PRESTO, JST, Japan*

Activation of growth factor receptors by ligand binding leads to an increased expression of *c-Myc*, a transcriptional regulator for cell proliferation. The activation of transcriptional factors via the activated receptors is thought to be the main role of *c-Myc* gene expression. We demonstrate here that epidermal growth factor receptor (EGFR)- and fibroblast growth factor receptor (FGFR)-mediated *c-Myc* induction and cell cycle progression in primary cultured mouse embryonic fibroblasts (MEFs) are abrogated by knockout of the *heparin-binding EGF-like growth factor* (*Hb-egf*) gene, or by a metalloproteinase inhibitor, although molecules downstream of the receptors are activated. Induction of *c-Myc* expression by EGF or basic FGF is recovered in *Hb-egf*-depleted MEFs by overexpression of wild-type proHB-EGF, but no recovery was observed with an uncleavable mutant of proHB-EGF. The uncleavable mutant also inhibited EGF-induced acetylation of histone H3 at the mouse *c-Myc* first intron region, which could negatively affect transcriptional activation. We conclude that signal transduction initiated by generation of the carboxyl-terminal fragment of proHB-EGF (HB-EGF-CTF) in the shedding event plays an important intermediary role between growth factor receptor activation and *c-Myc* gene induction.

J. Cell. Physiol. 214: 465–473, 2008.

Growth factors stimulate quiescent cells into DNA synthesis. The transcription factor encoded by the *c-Myc* gene is expressed in a strictly growth factor-dependent manner in quiescent cells (Obaya et al., 1999) and directs gene transcription associated with the transition from quiescence to proliferation. For example, *c-Myc* induces a number of target molecules involved in G1 phase entry into the cell cycle, including Cdc25A, cyclin D2, CDK4, Cul1, and E2F2 (Galaktionov et al., 1996; Leone et al., 1997; Bouchard et al., 1999; Hermeking et al., 2000), supporting the conclusion that *c-Myc* plays a central role in cell cycle progression as an upstream regulator of cell cycle regulatory molecules. Indeed, *c-Myc* null cells are able to survive, but display a marked lengthening of both the G1 and G2 phases of the cell cycle. Although the duration of S phase in *c-Myc* null cells remains unchanged, the G0 to S phase transition is also significantly delayed (Mateyak et al., 1997).

A key step for signaling through the epidermal growth factor receptor (EGFR) is the release of mature ligands such as heparin-binding EGF-like growth factor (HB-EGF) from their membrane-anchored precursor forms, a process referred to as "ectodomain shedding" (Blobel, 2005; Higashiyama and Nanba, 2005). The HB-EGF precursor (proHB-EGF) is cleaved by members of the "a disintegrin and metalloprotease" (ADAM) protease family (Asakura et al., 2002; Blobel, 2005; Higashiyama and Nanba, 2005), yielding the carboxyl terminal fragment of proHB-EGF (HB-EGF-CTF) in parallel with the production of HB-EGF. We have previously characterized HB-EGF-CTF as a novel intracellular signaling molecule that is acquired post-translationally and translocated into the nucleus, where it binds to and inactivates the promyelocytic leukemia zinc finger protein (PLZF) (Nanba et al., 2003). PLZF is a transcriptional repressor that suppresses transcription of genes such as *c-Myc*, *cyclin A2*, and *HoxD11* (Yeyati et al., 1999; Barna et al., 2000; McConnell et al., 2003). Thus, shedding of proHB-EGF participates in activation of two independent signal transduction pathways: signaling from EGFR after engagement of the shed growth factor, and a HB-EGF-CTF-mediated signaling (Higashiyama and Nanba, 2005). Here, we demonstrate that HB-EGF-CTF signaling is involved in growth factor-induced *c-Myc* expression.

Materials and Methods

Materials

12-o-tetradecanoylphorbol-13-acetate (TPA) was purchased from WAKO Pure Chem. Ind., Ltd. (Osaka, Japan). KB-R7785 (Asakura

Contract grant sponsor: Osaka Cancer Research Foundation.
Contract grant sponsor: Ehime University Research Foundation.
Contract grant sponsor: Ministry of Education, Culture, Sports, Science, and Technology of Japan;
Contract grant number: 17014068.
Contract grant sponsor: Precursory Research for Embryonic Science and Technology (Information and Cell Function);
Contract grant number: 17390081.

Daisuke Nanba's present address is Laboratory of Stem Cell Dynamics, School of Life Science, Swiss Federal Institute of Technology, Laussane, Switzerland.

*Correspondence to: Shigeki Higashiyama, Department of Biochemistry and Molecular Genetics, Ehime University Graduate School of Medicine, Shitsukawa, Toon, Ehime 791-0295, Japan.
E-mail: shigeki@m.ehime-u.ac.jp

Received 12 January 2007; Accepted 26 June 2007

DOI: 10.1002/jcp.21233

et al., 2002) and EGFR-neutralizing antibodies were obtained from Carna Biosciences, Inc. (Kobe, Japan) and Immuno-Biological Laboratories Co., Ltd. (Takasaki, Japan), respectively. Recombinant EGF and basic fibroblast growth factor (bFGF) were purchased from R&D Systems, Inc. (Minneapolis, MN).

Cell culture

The fibrosarcoma cell line HT1080 was cultured in Eagle minimum essential medium (EMEM) (Nikken Bio Medical Laboratory, Kyoto, Japan) with 10% fetal calf serum (FCS), 100 units of penicillin G potassium, and 100 μg of streptomycin sulfate per milliliter. The culture of primary human epidermal keratinocytes was prepared as described previously (Hashimoto et al., 1994). E13.5 embryos from loxHB-EGF mice were used to generate mouse embryonic fibroblasts (MEFs). MEFs were maintained in Dulbecco's modified Eagle medium (DMEM) (Nikken) supplemented with 10% FCS, 100 units of penicillin G potassium, and 100 μg of streptomycin sulfate per milliliter. Quiescent MEFs were prepared by serum starvation for 3 days. All cells were cultured in a humidified 37 C/ 5% CO_2 incubator.

Ribonuclease protection assay (RPA)

Total RNA was isolated from keratinocytes (1.0×10^6 cells) or MEFs (2.0×10^6 cells) with Trizol reagent (Invitrogen, Carlsbad, CA). Riboprobes were labeled with digoxigenin (DIG) using the DIG RNA labeling kit (Roche Diagnostics, Basel, Switzerland) according to the manufacturer's protocol. Thirty micrograms of total RNA harvested from cells cultured under each condition were hybridized with DIG-labeled probes. RNase treatment and gel resolution of protected probes were performed according to the manufacturer's protocol with the RPAIII kit (Ambion, Austin, TX). Each value (*c-Myc*/*Gapdh*) was normalized using the value for non-treated cells as taken to be one in each experiment. The values (means ± SD) were determined based on results in at least three independent experiments. *P*-values were obtained from Student's *t*-test.

Immunoprecipitation and immunoblotting

Immunoprecipitation and immunoblotting of cell lysates was performed as described previously (Goishi et al., 1995; Nanba et al., 2003). The primary antibodies used were as follows: mouse monoclonal antibodies to phospho-EGFR (Upstate, Billerica, MA); rabbit polyclonal antibodies to EGFR (Santa Cruz Biotechnology, Santa Cruz, CA), Erk1/2, phospho-Erk1/2 (Cell Signaling Technology, Lexington, KY), anti-β-actin (SIGMA, St. Louis, MO) and anti-HB-EGF-CTF antibodies (H1). Incubations of 1 h were performed with two secondary antibodies: HRP-conjugated goat anti-mouse and rabbit IgG (Promega, Madison, WI).

ProHB-EGF-AP shedding assay

HT1080 cells stably expressing alkaline phosphatase (AP)-tagged proHB-EGF (Asakura et al., 2002) were seeded in 24-well plates at a density of 1.0×10^5 cells per well and incubated for 24 h. Recombinant EGF (final 1–50 ng/ml), and bFGF (final 1–50 ng/ml) were added and the plates were incubated for a further 1 h. pAP-HB-EGF plasmids were transiently transfected into MEFs using a MEF Nucleofector kit (Amaxa Biosystems, Gaithersburg, MD). Twenty-four hours after transfection, the cells were treated with KB-R7785 (final 10–20 μM) and TPA (final 100 nM). Aliquots (100 μl each) of the conditioned media were used to measure AP activity as described previously (Tokumaru et al., 2000).

Immunofluorescence microscopy and visualization of the fluorescent signal intensity

Immunofluorescence microscopy of human keratinocytes using a rabbit polyclonal antibody to HB-EGF-CTF (Miyagawa et al., 1995) was performed as described previously (Nanba et al., 2003). We visualized the intensity of the fluorescent signal in each picture using Scion image (Scion Corporation, Frederick, MD).

Adenovirus construction and infection

Adenovirus vectors carrying genes encoding LacZ, green fluorescent protein (GFP), AP-tagged or non-tagged proHB-EGF, and uncleavable proHB-EGF were prepared using an adenovirus expression kit (Takara Biomedicals, Otsu Japan). An adenovirus expressing Cre recombinase (Kanegae et al., 1995) under the control of the CAG promoter (Niwa et al., 1991) was obtained from RIKEN BRC (Tsukuba, Japan). Purified, concentrated, and titer-checked viruses were applied to cells at a multiplicity of infection (MOI) of 100.

PCR, RT-PCR, and quantitative PCR analysis

Deletion of the mouse *Hb-egf* gene, mRNA expression of EGFR ligands, and *Plzf* in MEFs were confirmed by PCR and RT-PCR analysis, respectively. Primers are shown in Table 1. Quantitative PCR was performed using the ABI Prism 7700 sequencer detection system (Applied Biosystems, Foster, CA) with TaqMan Gene Expression Assay kits (Applied Biosystems) for mouse *c-Myc*

TABLE 1. Primer sequences for PCR and RT-PCR analysis

Primer	Sequence
loxHB-EGF (forward)	5'-CGGACAGTGCCTTAGTGGAACCTC-3'
loxHB-EGF (reverse)	5'-GCTTCTTCTTAGGAGGGAATCTTGGC-3'
Mouse *Hb-egf* (forward)	5'-TGCCGTCGGTGATGCTGAACT-3'
Mouse *Hb-egf* (reverse)	5'-GGTTCAGATCTGTCCCTTCCAAGTC-3'
Mouse *Tgf-α* (forward)	5'-GGAATTCCTAGCGCTGGGTATCCTGTTA-3'
Mouse *Tgf-α* (reverse)	5'-CAAGCTTACCACCACCAGGGCAGTGATG-3'
Mouse *Amphiregulin* (forward)	5'-GCAATTGTCATCAAGATTACTTTGG-3'
Mouse *Amphiregulin* (reverse)	5'-TCTGTTTCTCCTTCATATTCCCTG-3'
Mouse *Epiregulin* (forward)	5'-GGAATTCTGACGCTGCTTTGTCTAGGTT-3'
Mouse *Epiregulin* (reverse)	5'-CAAGCTTTATGCATCCAGCGGTTATGAT-3'
Mouse *Plzf* (forward)	5'-TCAAGAGCCACAAGCGCATCCACA-3'
Mouse *Plzf* (reverse)	5'-CGAGGCACCGTTGTGTGTTCTCA-3'
Mouse *GAPDH* (forward)	5'-CGTATTGGGCGCCTGGTCACCAG-3'
Mouse *GAPDH* (reverse)	5'-TCGCTCCTGGAAGATGGTGATGGG-3'
Region I (forward)	5'-GTGCAATGAGCTCGATGAAGGAAG-3'
Region I (reverse)	5'-GTCTTCTTATTCCGGACTCCTCG-3'
Region II (forward)	5'-TTACTGGACTGCGCAGGGAG-3'
Region II (reverse)	5'-CCACGTATACTTGGAGAGCCACTT-3'
Region III (forward)	5'-GGTAAGCACAGATCTGGTGGTCTT-3'
Region III (reverse)	5'-AAGTCAGAAGCTACGGAGCCTTCT-3'
Region IV (forward)	5'-GACGGCGCGAATAGGGAC-3'
Region IV (reverse)	5'-CTACTATCAGTGACGCTCGTCG-3'
zf5-binding region (forward)	5'-TATTGTGTGGAGCGAGGCAGCT-3'
zf5-binding region (reverse)	5'-GTGTAAACAGTAATAGCGCAGCATGAATTAAC-3'

mRNA. The values (means ± SD) were determined based on results in at least three independent experiments. *P*-values were obtained from Student's *t*-test.

Cell cycle analysis

Cell cycle analysis was performed as described previously (Nanba et al., 2003), using a FACScan instrument (Becton & Dickinson, Franklin Lakes, NJ).

Chromatin immunoprecipitation (ChIP) assay

Mock-treated or EGF-stimulated cells were formaldehyde crosslinked, harvested, and disrupted by Bioruptor (COSMOBIO, Tokyo, Japan), following the method in the EZ ChIP manual (Upstate). Immunoprecipitation was performed with anti-acetylated histone H3 (Upstate), anti-PLZF (Calbiochem, San Diego, CA), or anti-FLAG antibodies (SIGMA). The primers used in this assay are shown in Table I.

Results

Effect of cell growth factors on proHB-EGF shedding

Shedding of proHB-EGF occurs following stimulation by injury, UV, oxidants, phorbol esters, GPCR agonists, etc. (Takenobu et al., 2003; Higashiyama and Nanba, 2005). To investigate whether stimulation of growth factors such as EGF and bFGF induces shedding of proHB-EGF, we performed an AP-tagged assay with HT1080 cells that were stably transfected with AP-tagged proHB-EGF (Tokumaru et al., 2000). Increasing AP activity in the medium, indicating release of HB-EGF, was detected after stimulation of both EGF and bFGF (Fig. 1A). We also confirmed the production of HB-EGF-CTF after stimulation with these growth factors (Fig. 1B).
A metalloprotease inhibitor, KB-R7785, effectively blocked growth factor-induced proHB-EGF shedding, indicating involvement of metalloproteases in the shedding mechanism, as reported previously (Tokumaru et al., 2000; Nanba et al., 2003; Shirakata et al., 2005) (Fig. 1A). Moreover, we examined the localization of endogenous HB-EGF-CTF in human keratinocytes. Accumulation of endogenous HB-EGF-CTF in nuclei (Nanba et al., 2003) was markedly enhanced by the addition of bFGF, and this was inhibited by KB-R7785 (Fig. 2).

Effects of an inhibitor of proHB-EGF shedding on c-Myc expression induced by EGF

We have previously shown that HB-EGF-CTF, which is produced after shedding, regulates the expression of cyclin A2 by inhibition of the PLZF repressor protein (Nanba et al., 2003). PLZF has also been known to inhibit the expression of human *c-Myc* (McConnell et al., 2003). Therefore, we suspected that shedding of proHB-EGF and subsequent production of HB-EGF-CTF may control human *c-Myc* gene expression by abrogation of PLZF function. To examine the involvement of proHB-EGF shedding in EGF-induced *c-Myc* expression, we first performed an RPA with human primary cultured keratinocytes with intrinsic expression of HB-EGF, EGFR, and PLZF. Treatment with KB-R7785, a potent proHB-EGF shedding inhibitor (Asakura et al., 2002), resulted in a decreased expression of *c-Myc* mRNA under growth medium conditions (MDCB153 medium supplemented with insulin and bovine hypothalamic extract) to close to the basal level (Fig. 3A), whereas KB-R7785 did not affect phosphorylation of EGFR and Erk1/2, even when recombinant EGF was present (Fig. 3B). Treatment with a combination of KB-R7785 and anti-EGF receptor antibodies appeared to lead to even greater suppression of the *c-Myc* gene. These results imply that the activation of EGFR signaling brought about full induction of *c-Myc* expression with shedding of proHB-EGF.

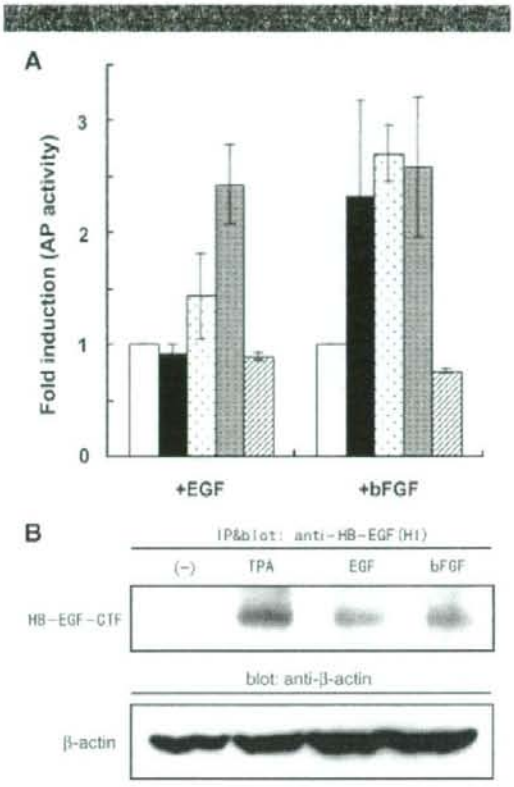

Fig. 1. Induction of proHB-EGF shedding by stimulation of EGF and bFGF. AP-tagged proHB-EGF was stably expressed in HT1080 fibrosarcoma cells. A: These cells were treated with various concentrations of EGF or bFGF for 1 h, and the AP activity was analyzed in each medium. Open bars, no stimulation; closed bars, 1 ng/ml; dotted bars, 10 ng/ml; shaded bars, 50 ng/ml; slashed bars, 50 ng/ml of growth factor and 10 μM of KB-R7785. All experiments were performed independently in triplicate. B: The lysates were collected from the above cells after each stimulation, and immunoprecipitated with anti-HB-EGF-CTF antibodies. After that, SDS-PAGE and immunoblotting with the above antibodies (upper part) were performed. β-actin in each cell lysate was detected with anti-β-actin antibodies as an indicator of protein loading (lower part).

To evaluate whether this event is species specific, we also examined expression of *c-Myc* in MEFs. mRNA of *c-Myc* was induced by stimulation of EGF and treatment with KB-R7785 partially suppressed *c-Myc* expression (Fig. 3C), but had no remarkable effect on phosphorylation of EGFR and Erk1/2 under treatment of KB-R7785 in MEFs (Fig. 3D). TPA is one of the strongest inducers of proHB-EGF shedding. To confirm the blocking effect of shedding by the metalloproteases inhibitor, KB-R7785, in MEFs, we performed proHB-EGF-AP shedding assay with adenovirus infection system (Fig. 3E). KB-R7785 even blocked the induction of proHB-EGF shedding by TPA.

Reduction of EGF-induced c-Myc gene expression in proHB-EGF-depleted mouse embryonic fibroblasts

To define the transcriptional regulation of *c-Myc* by HB-EGF more precisely, we generated *Hb-egf*-deficient MEFs using Cre/loxP technology (Fig. 4A). MEFs were isolated from loxHB-EGF

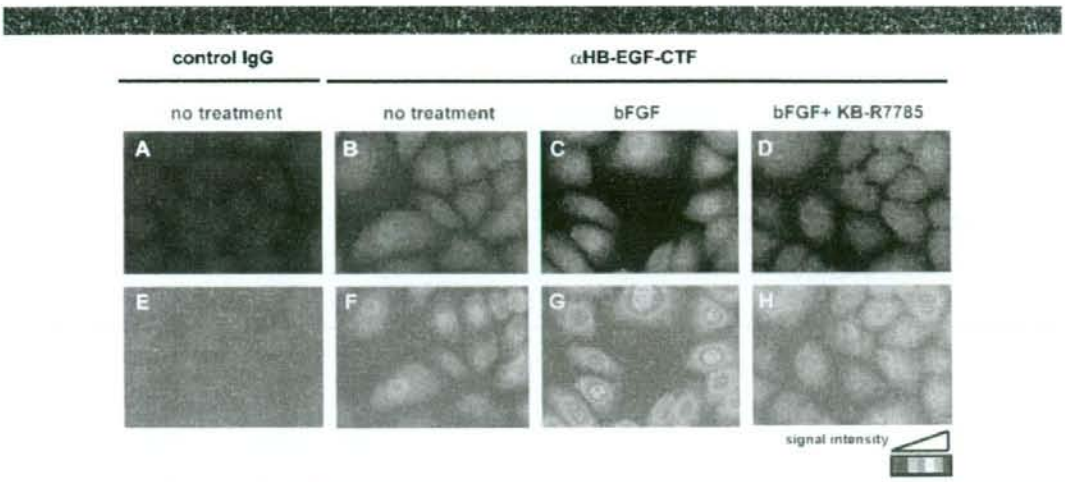

Fig. 2. Intracellular localization of endogenous HB-EGF-CTF in human keratinocytes, determined by fluorescent microscopy. Human keratinocytes were stimulated with 10 ng/ml bFGF for 30 min, after which they were fixed and stained with normal rabbit IgG or anti-HB-EGF-CTF antibodies. A, B, E, and F are images taken before stimulation; (C) and (G) are images collected after stimulation; and (D) and (H) show the effect of KB-R7785 treatment before stimulation with bFGF. A and E, normal rabbit IgG; B–D and F–H, anti-HB-EGF-CTF antibodies. Parts E–H show analytical data for A–D, respectively, determined using Scion Image.

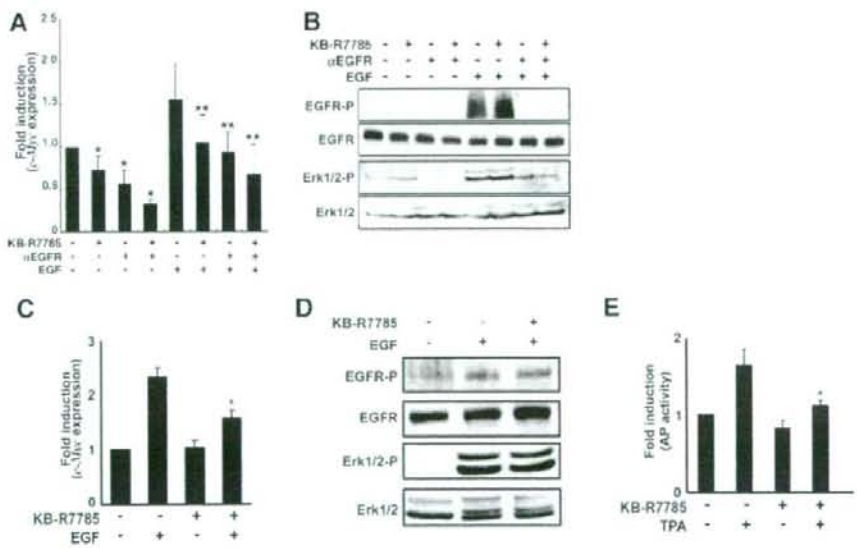

Fig. 3. Involvement of shedding of proHB-EGF in *c-Myc* transcription by human primary cultured keratinocytes and mouse embryonic fibroblasts. A: Analysis of *c-Myc* mRNA expression in keratinocytes by RPA. The intensities of the bands for *c-Myc* and *Gapdh* mRNA were measured by densitometry. In some cases, the keratinocytes were pretreated with 10 μM of KB-R7785 and/or 10 μg/ml of EGFR-neutralizing antibody for 1 h. Some of the cultures were further treated with 10 ng/ml of EGF for 1 h. Expression of *Gapdh* mRNA was examined as a control. $^{*}P < 0.05$ versus non-treated keratinocytes (lane 1) and $^{**}P < 0.05$ versus EGF-treated keratinocytes (lane 5). B: Phosphorylation of EGFR (middle parts) and Erk-1/-2 (lower parts) in keratinocytes was observed in a Western blot assay. C: Analysis of *c-Myc* mRNA expression in MEFs by RPA. The intensities of the bands for *c-Myc* and *Gapdh* mRNA were measured by densitometry. D : Detection of EGF signaling through the EGF receptor by an IP-Western assay. All experiments were performed independently in triplicate. E: Effect of KB-R7785 on shedding of proHB-EGF in MEFs. MEFs transiently expressed with AP-proHB-EGF were stimulated with 100 nM of 12-o-tetradecanoylphorbol-13-acetate (TPA). Before stimulation with TPA, the cells were treated with 20 μM of KB-R7785. $^{*}P < 0.05$ versus EGF-treated MEFs. A and C, The expression level of *c-Myc* was normalized using the level of *Gapdh*, and the fold induction is shown on the basis of the expression ratio relative to no treatment.

mice (Iwamoto et al., 2003; Shirakata et al., 2005) and infected with adenoviruses encoding either Cre or GFP. Deletion of the *Hb-egf* gene and the absence of its mRNA transcript were confirmed in Cre recombinase-expressing MEFs ($HB^{-/-}$ cells); in contrast, the gene and transcript were retained in GFP-expressing MEFs ($HB^{+/+}$ cells) (Fig. 4A–C). HB-EGF protein production in $HB^{+/+}$ and $HB^{-/-}$ cells was detected by Western blotting (Fig. 4B, lower part). Stimulation of EGF induced *c-Myc* expression in quiescent $HB^{+/+}$ cells, and up-regulation of *c-Myc* by EGF was also attenuated in $HB^{-/-}$ cells (Fig. 4D). Strikingly, phosphorylation of EGFR and Erk1/2 was stimulated equally in response to EGF in $HB^{+/+}$ and $HB^{-/-}$ cells (Fig. 4E).

Negative effects of uncleavable mutant of proHB-EGF on *c-Myc* gene expression and cell cycle progression

We next performed a recovery assay with adenovirus infection of MEFs to introduce exogenous expression of wild-type proHB-EGF. Protein production by wild-type or mutant proHB-EGF in $HB^{-/-}$ cells is shown in Fig. 5A. Infection with viruses carrying the wild-type protein restored *c-Myc* induction in $HB^{-/-}$ cells by EGF (Fig. 5B). Although the quiescent MEFs proceeded into S phase following EGF stimulation, entry into this phase was somewhat delayed in $HB^{-/-}$ cells compared to $HB^{+/+}$ cells with statistical significance (Fig. 5C). On the other hand, expression of an uncleavable mutant of proHB-EGF (Nanba et al., 2003) by adenovirus infection severely depressed *c-Myc* expression in both $HB^{-/-}$ and $HB^{+/+}$ cells (Fig. 5B). Moreover, adenovirus-driven overexpression of the uncleavable mutant completely inhibited cell cycle progression into S phase, although overproduction of wild-type proHB-EGF in $HB^{-/-}$ cells accelerated entry into S phase (Fig. 5C). It is presumably due to a potent dominant negative effect of the uncleavable form.

Elevated transcription of *c-Myc* was induced in quiescent MEFs stimulated with bFGF (Fig. 6A). The increased transcription of *c-Myc* mRNA in response to bFGF was significantly depressed in $HB^{-/-}$ cells (Fig. 6A). Expression of wild-type proHB-EGF recovered the induction of the *c-Myc* gene by bFGF in $HB^{-/-}$ cells, but expression of the uncleavable mutant of proHB-EGF did not do so (Fig. 6B). These data raise the possibility that the release of overexpressed HB-EGF restored *c-Myc* induction by bFGF. However, induction by bFGF was not inhibited by treatment with HB-EGF-neutralizing antibodies under the expression of proHB-EGF (Fig. 6B). bFGF induced quiescent MEFs into S phase, but S phase entry was delayed in $HB^{-/-}$ cells compared to $HB^{+/+}$ cells (Fig. 6C). Furthermore, expression of the uncleavable mutant markedly suppressed S phase entry, similarly to the result with EGF.

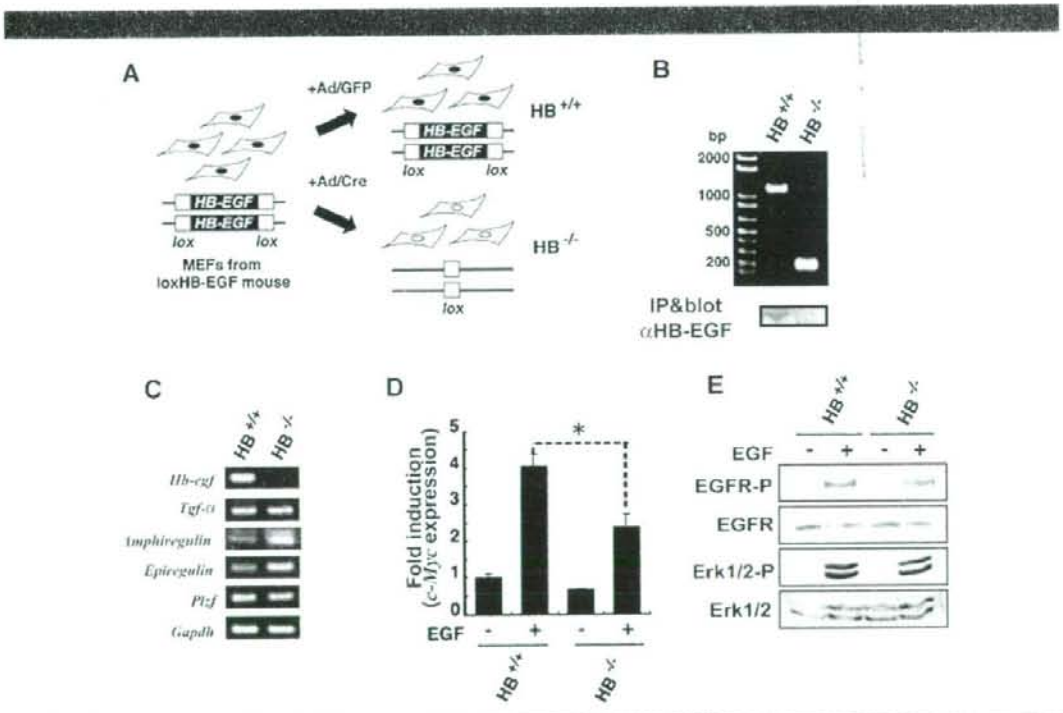

Fig. 4. Involvement of HB-EGF in *c-Myc* transcription induced by EGFR signaling. A: Schematic representation of generation of proHB-EGF-deficient MEFs from loxHB-EGF mice. B: The upper part shows PCR detection of the *Hb-egf* gene in loxHB-EGF MEFs after infection with adenoviruses expressing GFP ($HB^{+/+}$) or Cre ($HB^{-/-}$). The upper band represents the intact *Hb-egf* gene flanked by *loxP* sites, and the lower band reflects the fragment size decrease after *Hb-egf* gene deletion. The bottom part shows the protein level of proHB-EGF in each type of cell. Data were collected for 10^4 cells for each condition. C: RT-PCR analysis of mRNAs for EGFR ligands (*Hb-egf*, *Tgf-α*, *Amphiregulin*, and *Epiregulin*) and *Plzf* mRNA expression. D: Analysis of *c-Myc* mRNA expression in $HB^{+/+}$ and $HB^{-/-}$ cells by quantitative PCR analysis. Serum-starved MEFs were stimulated with 10 ng/ml EGF for 1 h. Expression of *Gapdh* mRNA was examined as a normalization control, and densitometric analysis was performed. $^*P < 0.05$ versus $HB^{+/+}$ cells treated with EGF. E: Phosphorylation of EGFR and Erk1/2 induced by addition of EGF for 15 min in $HB^{+/+}$ and $HB^{-/-}$ cells. All experiments were performed independently in triplicate.

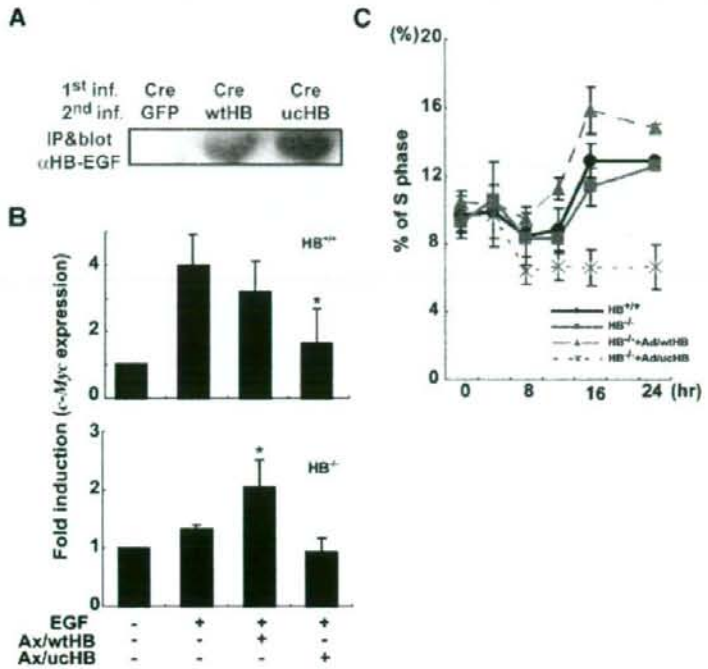

Fig. 5. EGFR signaling-induced *c-Myc* transcription and cell cycle progression by expression of proHB-EGF and an uncleavable mutant. A: The protein level of each proHB-EGF in adenovirus-infected cells. Immunoprecipitation and the Western blotting assay were each performed using 10^6 cells. 1st inf. and 2nd inf. indicate first and second infection respectively. B: RPA of *c-Myc* transcription induced by EGF in $HB^{+/+}$ and $HB^{-/-}$ cells infected with adenoviruses encoding either proHB-EGF (Ax/wtHB) or its uncleavable mutant (Ax/ucHB). The expression level of *c-Myc* was normalized using the corresponding expression level of *Gapdh*, and fold induction is shown based on a control value of 1. C: Flow cytometry analysis of cell cycle progression in cells stimulated with EGF. All experiments were performed independently in triplicate.

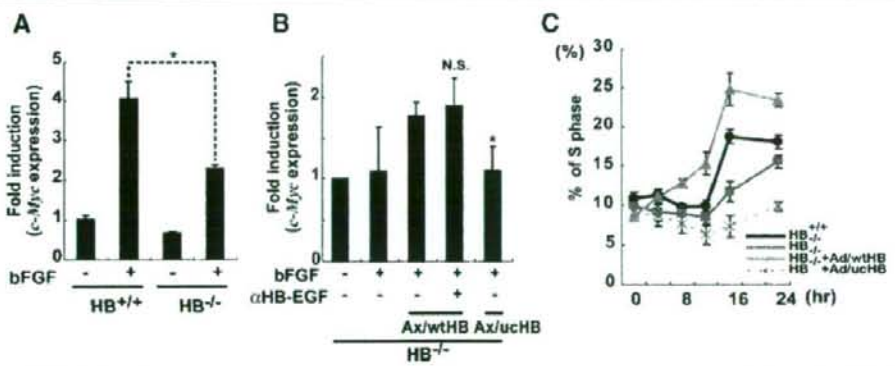

Fig. 6. Involvement of proHB-EGF shedding in *c-Myc* transcription induced by bFGF. A: Quantitative PCR analysis of *c-Myc* transcription induced by bFGF in $HB^{+/+}$ and $HB^{-/-}$ cells. Serum-starved MEFs were stimulated with 1 ng/ml bFGF for 1 h. Expression of *Gapdh* mRNA was examined as a control. B: RPA of *c-Myc* transcription induced by bFGF in $HB^{-/-}$ cells infected with Ax/wtHB and Ax/ucHB. A HB-EGF-neutralizing antibody (αHB-EGF) was used to inhibit the function of mature HB-EGF. The expression level of *c-Myc* was normalized using the corresponding expression level of *Gapdh*, and fold induction is shown based on a control value of 1. C: Flow cytometry analysis of cell cycle progression in cells stimulated with bFGF. $^*P < 0.05$ versus $HB^{+/+}$ cells. All experiments were performed independently in triplicate.

These results suggest that proHB-EGF shedding and subsequent HB-EGF-CTF signaling can modulate bFGF signaling-induced *c-Myc* expression and cell cycle progression.

Epigenetic effect of uncleavable proHB-EGF on Mouse *c-Myc* gene promoter

We have previously reported that HB-EGF-CTF inactivates PLZF, a transcriptional repressor, by induction of translocation to the cytoplasm. On the other hand, a recent study has shown that PLZF represses expression of human *c-Myc* (McConnell et al., 2003). When we checked the PLZF-binding motifs in the 5 kb region from the transcriptional start site of the mouse *c-Myc* gene, six putative sites were found (Fig. 7A). To examine chromatin modification in MEFs infected by adenoviruses carrying GFP or the uncleavable mutant of proHB-EGF, a chromatin immunoprecipitation (ChIP) assay was performed. After stimulation with EGF, the level of acetylated histone H3 increased at the region III (Fig. 7B), where the acetylation, however, was not induced with expression of the uncleavable form of proHB-EGF. These data suggest that production of HB-EGF-CTF followed by shedding is required for histone modification. We also examined the participation of PLZF in this region in the ChIP assay. However, the fragment of the region III was not detected with anti-PLZF antibodies (data not shown). We also tried detection of this region with anti-FLAG antibodies in FLAG-tagged PLZF-overexpressed cells, but the region III was not detected again (Fig. 7C).

Discussion

Induction of *c-Myc* transcription by receptor tyrosine kinases (RTKs) is regulated by at least two distinct intracellular signaling pathways: the Ras/Raf/MEK/ERK (MAPK) pathway (Kerkhoff et al., 1998) and the Src pathway (Barone and Courtneidge, 1995; Chiariello et al., 2001). The MAPK pathway induces proHB-EGF shedding by the activation of metalloproteases (Gechtman et al., 1999; Umata et al., 2001). The activated metalloproteases cleave proHB-EGF at the plasma membrane, generating both the EGFR ligand HB-EGF and the transcription-modulating protein HB-EGF-CTF (Nanba et al., 2003). The present study demonstrates that signal transduction mediated by HB-EGF-CTF modulates induction of *c-Myc* transcription and cell cycle progression by EGF and bFGF.

Reiss et al. provided evidence that proteolysis of transmembrane proteins on the cell surface is involved in *c-Myc* expression, by showing decreased expression of *c-Myc* in ADAM10-deficient MEFs (Reiss et al., 2005). ADAM10 cleaves N-cadherin, an event that causes redistribution of β-catenin from the plasma membrane to the cytoplasmic pool, thereby accelerating β-catenin/Tcf signaling and the resulting *c-Myc* expression (He et al., 1998). ADAM10 is also a sheddase for proHB-EGF and other EGFR ligand precursors (Sahin et al., 2004). Therefore, it is possible that KB-R7785, a metalloproteinase inhibitor, could inhibit the increase in *c-Myc* expression by blocking redistribution of β-catenin (Fig. 3A, C). However, expression of the *c-Myc* gene by growth factors diminished in MEFs in which the *Hb-egf* gene was removed by Cre recombinase (Figs. 4D, 5B, and 6A). Moreover, expression of an uncleavable mutant of proHB-EGF did not recover expression of *c-Myc*, rather inhibited it (Figs. 5B and 6B), suggesting that full induction of the *c-Myc* gene by growth factors requires shedding of proHB-EGF. CTF signaling derived from proHB-EGF may also contribute to *c-Myc* transcription induced by growth factors.

c-Myc participates in a variety of biological processes, including cell proliferation, differentiation, apoptosis, metabolism, and tumorigenesis (Dang, 1999; Murphy et al., 2005). We performed cell cycle analysis to determine the effects caused by a change in *c-Myc* expression. Delayed S phase entry was observed in *Hb-egf*-depleted MEFs following stimulation with either EGF or bFGF (Figs. 5C and 6C). Expression of the uncleavable mutant of proHB-EGF in the presence of the wild-type protein completely stopped the cell

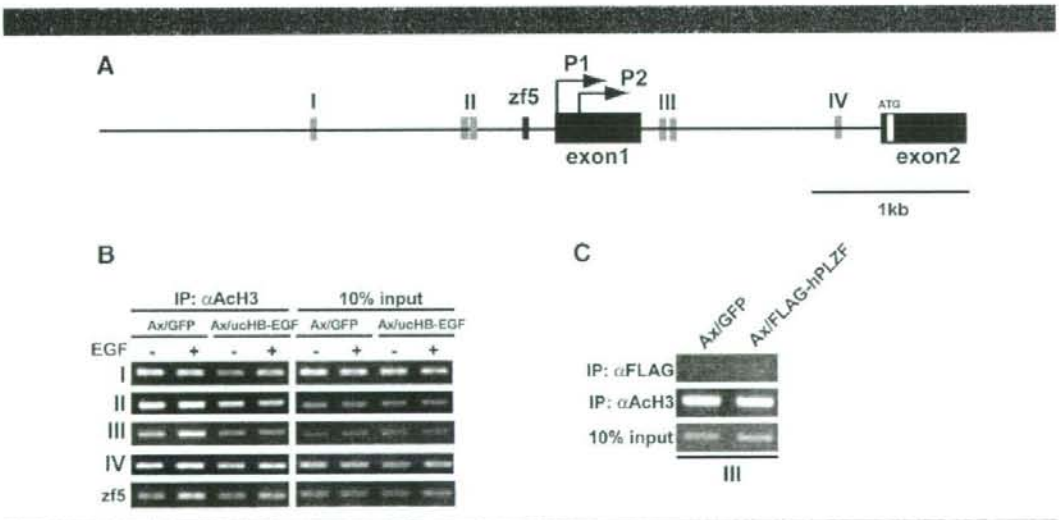

Fig. 7. Inhibition of EGF-induced acetylation of histone H3 at the mouse *c-Myc* intron I by the uncleavable mutant of proHB-EGF. A: Schematic diagram of the *c-Myc* promoter, exon I, intron I, and exon II. Gray boxes show the PLZF-binding motif-like sites. The regions including gray boxes are named as regions I, II, III, and IV; zf5 indicates the binding motif of ZF5, a novel *c-Myc* suppressor; black boxes indicate exons; and P1 and P2 are transcriptional start sites. B: ChIP assay with MEFs infected by adenoviruses including cDNA of GFP or the uncleavable mutant of proHB-EGF, and PLZF (C). All experiments were performed independently in triplicate.

cycle. These results indicate that the shedding event of proHB-EGF is one of the important steps to regulate cell cycle progression, even in the presence of growth factors. Therefore, the present study raises a possibility that cellular behavior involving *c-Myc* expression is controlled by regulating proteolysis of cell surface proteins and signaling by their cell-associated remnant fragments.

Our current studies indicate that the CTFs of other EGF family members such as amphiregulin, TGF-α, and epiregulin bind to PLZF as well as HB-EGF does (unpublished work, Morimoto and Higashiyama), and that these members share shedding enzymes in some extent (Sahin et al., 2004). The former supports the idea that CTF signaling would be redundant in some members of the EGF family for explaining that the lack of HB-EGF-CTF showed partial inhibition of *c-Myc* induction by EGF and bFGF. The latter indicates that overexpression of uncleavable proHB-EGF would competitively block the shedding of other members in the EGF family and works as a dominant negative form, explaining that uncleavable proHB-EGF markedly blocked S phase entry of cell cycle induced by EGF and bFGF.

Stimulation of EGF enhanced acetylation of histone H3 at the keratin 16 and c-fos chromatin promoter (Cheung et al., 2000; Wang et al., 2006). We also observed enhanced levels of acetylated histone H3 with EGF treatment in the mouse *c-Myc* intron I near the boundary of the exon I (Fig. 7B). The activated *c-Myc* allele in Burkitt's lymphoma is associated with a cluster of somatic mutations within a discrete domain of intron I that define protein recognition sequences, designated as *c-Myc* intron factors (MIFs) (Zajac-Kaye and Levens, 1990; Tachibana et al., 1993; Yu et al., 1993). The sequence of the intron I in the mouse *c-Myc* gene is partly homologous to that in the human *c-Myc*, and this region could also be important in the regulation of the expression of *c-Myc* in mouse.

PLZF negatively regulates the human *cyclin A2* and *c-Myc* genes (Yeyati et al., 1999; McConnell et al., 2003) and the consensus binding sequence has been identified. We have recently reported that HB-EGF-CTF targets PLZF to de-repress the human *cyclin A2* gene (Nanba et al., 2003). It was shown here that shedding of proHB-EGF and sequential production of HB-EGF-CTF affected activation of *c-Myc* in MEFs, and PLZF may participate in this event. However, over-expression of PLZF did not result in attenuation of acetylation of histone H3 at the intron I region, which includes two similar PLZF-binding motif sites (Fig. 7C). Moreover, we tested the influence of ZF5, a novel regulatory factor for *c-Myc* expression (Numoto et al., 1993), which has a binding site in the upper region of exon I (Fig. 7A). However, no effects of the uncleavable proHB-EGF mutant were observed at this region in the ChIP assay (Fig. 7B). These results raise the possibility that other C_2H_2 type zinc finger transcriptional repressors with similar features to PLZF might be targeted by HB-EGF-CTF in the expression of mouse *c-Myc*. This speculation might be supported by two pieces of the following important information. (1) HB-EGF-CTF is able to bind Bcl6, a PLZF-like transcriptional repressor (Kinugasa et al., 2007). (2) PLZF-like repressors (Kruppel-type zinc finger repressors) are well-known gene family showing that active rounds of segmental duplication, involving single genes or larger regions and including both tandem and distributed duplication events, have driven the expansion of this mammalian gene family. Comparisons between the human genes and ZNF loci mined from the draft mouse, dog, and chimpanzee genomes highlighted a substantial level of lineage-specific change. Kruppel-type zinc finger genes are widely expressed and clustered genes are typically not coregulated, indicating that paralogs have evolved to fill roles in many different biological processes in each species (Huntley et al., 2006).

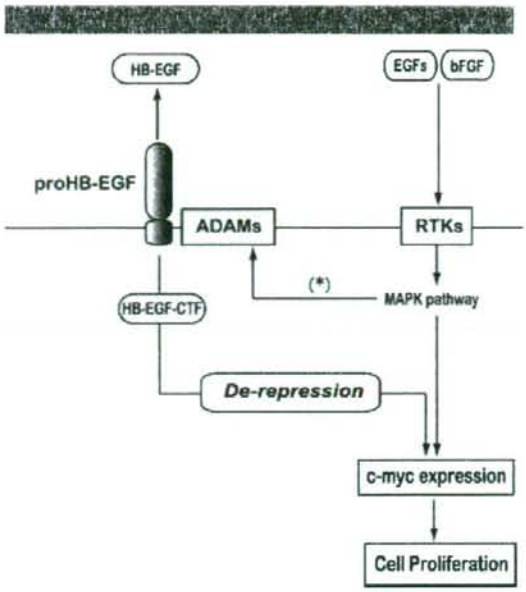

Fig. 8. A schematic diagram for the proposed role of HB-EGF-CTF signaling in c-Myc transcription induced by growth factor receptor activation. (*) Activation of ADAMs by MAPK pathway has already been reported (Gechtman et al., 1999; Umata et al., 2001).

In conclusion, we have shown here that shedding of proHB-EGF induces epigenetic changes in the mouse *c-Myc* gene, in support of the induction of expression of *c-Myc* by EGF or bFGF. HB-EGF-CTF may target other transcriptional repressors besides PLZF, and further studies are required to identify the target repressors. We propose a possible model for the mechanism of *c-Myc* regulation by RTKs in Figure 8.

Acknowledgments

We thank Dr. I. Saito for the Cre-expressing adenovirus, Dr. J. Miyazaki for the CAG promoter, Drs. S. Yamazaki and E. Mekada for technical advice about loxHB-EGF mice, Drs. H. Ohmoto and K. Yoshino for adenovirus construction and providing KB-R7785, and Dr. S. Tokumaru, Dr. N. Matsushita, Dr. F. Shiba, Mr. H. Nakayama, Ms. T. Tsuda, and Ms. E. Tan for technical assistance. We are also grateful to Dr. J. A. Abraham for editing the article. This work was supported by a research grant to D. N. from Osaka Cancer Research Foundation, Ehime University Research Foundation, and Grants-in-aid for Scientific Research to S. H. from the Ministry of Education, Culture, Sports, Science, and Technology of Japan, and Precursory Research for Embryonic Science and Technology (Information and Cell Function) (no.17014068, 17390081).

Literature Cited

Asakura M, Kitakaze M, Takashima S, Liao Y, Ishikura F, Yoshinaka T, Ohmoto H, Node K, Yoshino K, Ishiguro H, Asanuma H, Sanada S, Matsumura Y, Takeda H, Beppu S, Tada M, Hori M, Higashiyama S. 2002. Cardiac hypertrophy is inhibited by antagonism of ADAM12 processing of HB-EGF: Metalloproteinase inhibitors as a new therapy. Nat Med 8:35–40.

Barna M, Hawe N, Niswander L, Pandolfi PP. 2000. Plzf regulates limb and axial skeletal patterning. Nat Genet 25:166–172.

Barone MV, Courtneidge SA. 1995. Myc but not Fos rescue of PDGF signalling block caused by kinase-inactive Src. Nature 378:509–512.

Blobel CP. 2005. ADAMs: Key components in EGFR signalling and development. Nat Rev Mol Cell Biol 6:32–43.

Bouchard C, Thieke K, Maier A, Saffrich R, Hanley-Hyde J, Ansorge W, Reed S, Sicinski P, Bartek J, Eilers M. 1999. Direct induction of cyclin D2 by Myc contributes to cell cycle progression and sequestration of p27. EMBO J 18:5321–5333.
Cheung P, Tanner KG, Cheung WL, Sassone-Corsi P, Denu JM, Allis CD. 2000. Synergistic coupling of histone H3 phosphorylation and acetylation in response to epidermal growth factor stimulation. Mol Cell 5:905–915.
Chiariello M, Marinissen MJ, Gutkind JS. 2001. Regulation of c-myc expression by PDGF through Rho GTPases. Nat Cell Biol 3:580–586.
Dang CV. 1999. c-Myc target genes involved in cell growth, apoptosis, and metabolism. Mol Cell Biol 19:1–11.
Galaktionov K, Chen X, Beach D. 1996. Cdc25 cell-cycle phosphatase as a target of c-myc. Nature 382:511–517.
Gechtman Z, Alonso JL, Raab G, Ingber DE, Klagsbrun M. 1999. The shedding of membrane-anchored heparin-binding epidermal-like growth factor is regulated by the Raf/mitogen-activated protein kinase cascade and by cell adhesion and spreading. J Biol Chem 274:28828–28835.
Goishi K, Higashiyama S, Klagsbrun M, Nakano N, Umata T, Ishikawa M, Mekada E, Taniguchi N. 1995. Phorbol ester induces the rapid processing of cell surface heparin-binding EGF-like growth factor: Conversion from juxtacrine to paracrine growth factor activity. Mol Biol Cell 6:967–980.
Hashimoto K, Higashiyama S, Asada H, Hashimura E, Kobayashi T, Sudo K, Nakagawa T, Damm D, Yoshikawa K, Taniguchi N. 1994. Heparin-binding epidermal growth factor-like growth factor is an autocrine growth factor for human keratinocytes. J Biol Chem 269:20060–20066.
He TC, Sparks AB, Rago C, Hermeking H, Zawel L, da Costa LT, Morin PJ, Vogelstein B, Kinzler KW. 1998. Identification of c-MYC as a target of the APC pathway. Science 281:1509–1512.
Hermeking H, Rago C, Schuhmacher M, Li Q, Barrett JF, Obaya AJ, O'Connell BC, Mateyak MK, Tam W, Kohlhuber F, Dang CV, Sedivy JM, Eick D, Vogelstein B, Kinzler KW. 2000. Identification of CDK4 as a target of c-MYC. Proc Natl Acad Sci USA 97:2229–2234.
Higashiyama S, Nanba D. 2005. ADAM-mediated ectodomain shedding of HB-EGF in receptor cross-talk. Biochim Biophys Acta 1751:110–117.
Huntley S, Baggott DM, Hamilton AT, Tran-Gyamfi M, Yang S, Kim J, Gordon L, Branscomb E, Stubbs L. 2006. A comprehensive catalog of human KRAB-associated zinc finger genes: Insights into the evolutionary history of a large family of transcriptional repressors. Genome Res 16:669–677.
Iwamoto R, Yamazaki S, Asakura M, Takashima S, Hasuwa H, Miyado K, Adachi S, Kitakaze M, Hashimoto K, Raab G, Nanba D, Higashiyama S, Hori M, Klagsbrun M, Mekada E. 2003. Heparin-binding EGF-like growth factor and ErbB signaling is essential for heart function. Proc Natl Acad Sci USA 100:3221–3226.
Kanegae Y, Lee G, Sato Y, Tanaka M, Nakai M, Sakaki T, Sugano S, Saito I. 1995. Efficient gene activation in mammalian cells by using recombinant adenovirus expressing site-specific Cre recombinase. Nucleic Acids Res 23:3816–3821.
Kerkhoff E, Houben R, Loffler S, Troppmair J, Lee JE, Rapp UR. 1998. Regulation of c-myc expression by Ras/Raf signalling. Oncogene 16:211–216.
Kinugasa Y, Hieda M, Hori M, Higashiyama S. 2007. The carboxyl-terminal fragment of Pro-HB-EGF reverses Bcl6-mediated gene repression. J Biol Chem 282:14797–14806.
Leone G, DeGregori J, Sears R, Jakoi L, Nevins JR. 1997. Myc and Ras collaborate in inducing accumulation of active cyclin E/Cdk2 and E2F. Nature 387:422–426.
Mateyak MK, Obaya AJ, Adachi S, Sedivy JM. 1997. Phenotypes of c-Myc-deficient rat fibroblasts isolated by targeted homologous recombination. Cell Growth Differ 8:1039–1048.
McConnell MJ, Chevallier N, Berkofsky-Fessler W, Giltnane JM, Malani RB, Staudt LM, Licht JD. 2003. Growth suppression by acute promyelocytic leukemia-associated protein PLZF is mediated by repression of c-myc expression. Mol Cell Biol 23:9375–9388.
Miyagawa J, Higashiyama S, Kawata S, Inui Y, Tamura S, Yamamoto K, Nishida M, Nakamura T, Yamashita S, Matsuzawa Y, Taniguchi N. 1995. Localization of heparin-binding EGF-like growth factor in the smooth muscle cells and macrophages of human atherosclerotic plaques. J Clin Invest 95:404–411.
Murphy MJ, Wilson A, Trumpp A. 2005. More than just proliferation: Myc function in stem cells. Trends Cell Biol 15:128–137.
Nanba D, Mammoto A, Hashimoto K, Higashiyama S. 2003. Proteolytic release of the carboxy-terminal fragment of proHB-EGF causes nuclear export of PLZF. J Cell Biol 163:489–502.
Niwa H, Yamamura K, Miyazaki J. 1991. Efficient selection for high-expression transfectants with a novel eukaryotic vector. Gene 108:193–199.
Numoto M, Niwa O, Kaplan J, Wong KK, Merrell K, Kamiya K, Yanagihara K, Calame K. 1993. Transcriptional repressor ZF5 identifies a new conserved domain in zinc finger proteins. Nucleic Acids Res 21:3767–3775.
Obaya AJ, Mateyak MK, Sedivy JM. 1999. Mysterious liaisons: The relationship between c-Myc and the cell cycle. Oncogene 18:2934–2941.
Reiss K, Maretzky T, Ludwig A, Tousseyn T, de Strooper B, Hartmann D, Saftig P. 2005. ADAM10 cleavage of N-cadherin and regulation of cell-cell adhesion and beta-catenin nuclear signalling. EMBO J 24:742–752.
Sahin U, Weskamp G, Kelly K, Zhou HM, Higashiyama S, Peschon J, Hartmann D, Saftig P, Blobel CP. 2004. Distinct roles for ADAM10 and ADAM17 in ectodomain shedding of six EGFR ligands. J Cell Biol 164:769–779.
Shirakata Y, Kimura R, Nanba D, Iwamoto R, Tokumaru S, Morimoto C, Yokota K, Nakamura M, Sayama K, Mekada E, Higashiyama S, Hashimoto K. 2005. Heparin-binding EGF-like growth factor accelerates keratinocyte migration and skin wound healing. J Cell Sci 118:2363–2370.
Tachibana K, Takayama N, Matsuo K, Kato S, Yamamoto K, Ohyama K, Umezawa A, Takano T. 1993. Allele-specific activation of the c-myc gene in an atypical Burkitt's lymphoma carrying the t(2;8) chromosomal translocation 250 kb downstream from c-myc. Gene 124:231–237.
Takenobu H, Yamazaki A, Hirata M, Umata T, Mekada E. 2003. The stress- and inflammatory cytokine-induced ectodomain shedding of heparin-binding epidermal growth factor-like growth factor is mediated by p38 MAPK, distinct from the 12-O-tetradecanoylphorbol-13-acetate- and lysophosphatidic acid-induced signaling cascades. J Biol Chem 278:17255–17262.
Tokumaru S, Higashiyama S, Endo T, Nakagawa T, Miyagawa JI, Yamamori K, Hanakawa Y, Ohmoto H, Yoshino K, Shirakata Y, Matsuzawa Y, Hashimoto K, Taniguchi N. 2000. Ectodomain shedding of epidermal growth factor receptor ligands is required for keratinocyte migration in cutaneous wound healing. J Cell Biol 151:209–220.
Umata T, Hirata M, Takahashi T, Ryu F, Shida S, Takahashi Y, Tsuneoka M, Miura Y, Masuda M, Horiguchi Y, Mekada E. 2001. A dual signaling cascade that regulates the ectodomain shedding of heparin-binding epidermal growth factor-like growth factor. J Biol Chem 276:30475–30482.
Wang YN, Chen YJ, Chang WC. 2006. Activation of extracellular signal-regulated kinase signaling by epidermal growth factor mediates c-Jun activation and p300 recruitment in keratin 16 gene expression. Mol Pharmacol 69:85–98.
Yeyati PL, Shaknovich R, Boterashvili S, Li J, Ball HJ, Waxman S, Nason-Burchenal K, Dmitrovsky E, Zelent A, Licht JD. 1999. Leukemia translocation protein PLZF inhibits cell growth and expression of cyclin A. Oncogene 18:925–934.
Yu BW, Ichinose I, Bonham MA, Zajac-Kaye M. 1993. Somatic mutations in c-myc intron I cluster in discrete domains that define protein binding sequences. J Biol Chem 268:19586–19592.
Zajac-Kaye M, Levens D. 1990. Phosphorylation-dependent binding of a 138-kDa myc intron factor to a regulatory element in the first intron of the c-myc gene. J Biol Chem 265:4547–4551.

Journal of Dermatological Science (2008) 50, 53–60

ELSEVIER

Dermatological SCIENCE

www.intl.elsevierhealth.com/journals/jods

PPARγ is an important transcription factor in 1α,25-dihydroxyvitamin D3-induced involucrin expression

Xiuju Dai, Koji Sayama*, Yuji Shirakata, Sho Tokumaru, Lujun Yang, Mikiko Tohyama, Satoshi Hirakawa, Yasushi Hanakawa, Koji Hashimoto

Department of Dermatology, Ehime University School of Medicine, Ehime, Japan

Received 12 June 2007; received in revised form 18 September 2007; accepted 26 October 2007

KEYWORDS
1α,25-Dihydroxyvitamin D3;
PPARγ;
Involucrin;
AP-1;
p38

Summary

Background: 1α,25-Dihydroxyvitamin D3 ($1\alpha,25(OH)_2D_3$), the active form of vitamin D, suppresses keratinocyte proliferation, promotes keratinocyte differentiation, and induces involucrin expression. Peroxisome proliferation-activated receptors (PPARs) are ligand-activated transcription factors. It has been reported that PPARs stimulate keratinocyte differentiation and regulate the expression of differentiation molecules.
Objective: Keratinocytes treated with $1\alpha,25(OH)_2D_3$ induced PPARγ, which was followed by increased involucrin expression. In this study, we investigated whether PPARγ is involved in the $1\alpha,25(OH)_2D_3$-induced involucrin expression in human keratinocytes.
Methods: Subconfluent keratinocytes were treated with 10^{-7} M $1\alpha,25(OH)_2D_3$ for the indicated times, and PPAR and involucrin mRNA expression were determined by real-time RT-PCR. The levels of PPARs, involucrin, p38, and phospho-p38 proteins were assayed by Western blotting, and the DNA binding activities of PPARγ and AP-1 were investigated by electrophoretic mobility shift assays (EMSA). To examine the role of PPARγ in $1\alpha,25(OH)_2D_3$ responses, recombinant adenovirus carrying a dominant-negative form of PPARγ (Axdn-PPARγ) was constructed and transfected into keratinocytes. The p38 inhibitor SB203580 was added to the cultures to evaluate the involvement of p38 in involucrin expression.
Results: $1\alpha,25(OH)_2D_3$ induced PPARγ expression and stimulated PPARγ activity. The introduction of dn-PPARγ inhibited the expression of involucrin mRNA and protein induced by $1\alpha,25(OH)_2D_3$, and suppressed AP-1 DNA binding activity. $1\alpha,25(OH)_2D_3$

Abbreviations: $1\alpha,25(OH)_2D_3$, 1α,25-dihydroxyvitamin D3; AP-1, activator protein-1; Ax, adenovirus vector; m.o.i., multiplicity of infection; PPAR, peroxisome proliferator-activated receptor; VDR, vitamin D receptor; VDRE, vitamin D response elements.

* Corresponding author. Tel.: +81 89 960 5350; fax: +81 89 960 5352.
E-mail address: sayama@m.ehime-u.ac.jp (K. Sayama).

doi:10.1016/j.jdermsci.2007.10.011

also triggered the phosphorylation of p38, which contributes to involucrin induction. Moreover, dn-PPARγ prevented the $1\alpha,25(OH)_2D_3$-induced phosphorylation of p38.
Conclusions: These results suggest that PPARγ regulates involucrin expression by controlling the AP-1 signal and p38 activation in $1\alpha,25(OH)_2D_3$-induced keratinocyte differentiation.

1. Introduction

Within the epidermis, keratinocytes migrate from the proliferative basal compartment to the upper, terminally differentiated, cornified layers of the skin, passing through a series of differentiation stages characterized by the expression of specific marker genes [1]. As involucrin is a major component of the cornified envelope, and its expression in the epidermis is tightly linked to the status of keratinocytes differentiation, involucrin is a widely used marker for keratinocyte differentiation. The activity of the involucrin promoter is complex and cell type-specific.

$1\alpha,25(OH)_2D_3$ is a hormonally active form of vitamin D, and its cellular functions are usually mediated through the nuclear hormone receptor, VDR, which binds as a heterodimer with the retinoid X receptor (RXR) to the vitamin D response element (VDRE) in the promoter region of vitamin D-responsive genes [2]. Studies have shown that $1\alpha,25(OH)_2D_3$ induces the terminal differentiation of preconfluent cultured human keratinocytes, together with elevated expression of involucrin and formation of cornified envelope [3].

PPARs are transcription factors belonging to the ligand-activated nuclear hormone receptor superfamily. On binding ligands, PPARs form heterodimers with RXR to facilitate the transcription of target genes involved in many cellular functions, including epidermal differentiation and barrier formation [4,5]. All of the PPAR superfamily members (e.g., PPARα, PPARβ/δ, and PPARγ) have been identified in keratinocytes [6], and the activation of PPARs regulate the expression of several differentiation markers [5,7]. PPARγ ligands appear to regulate cellular differentiation and cutaneous homeostasis, similar to other nuclear hormones such as glucocorticoids, retinoids, and vitamin D [8,9]. Here, we show that PPARγ signal is involved in $1\alpha,25(OH)_2D_3$-induced involucrin expression in human keratinocytes, by regulating AP-1 transactivation and p38 activity. This report suggests a vital role for PPARγ in the $1\alpha,25(OH)_2D_3$ response of cultured differentiating human keratinocytes.

2. Materials and methods

2.1. Keratinocyte culture

Primary normal human keratinocytes were isolated from surgically discarded neonatal skin samples. This study was conducted according to the Declaration of Helsinki Principles, and all of the procedures that involved human subjects received prior approval from the Ethics Committee at the Ehime University School of Medicine, Japan. Written consent was provided by patient guardian before experiments were initiated. Normal human keratinocytes were cultured in MCDB153 medium as described previously [10].

2.2. Adenovirus vector construction and infection

The pcDNA3 expression vector expressing flag-tagged L468A/E471A PPARγ (dn-PPARγ) was a gift from Professor Chatterjee (University of Cambridge, UK). This double-mutant form of PPARγ exhibits impaired transcriptional activity, silences basal transcription, and is a potent dominant-negative inhibitor of wild-type PPARγ activity [11]. Adenovirus vector (Ax) containing dn-PPARγ was generated and transfected into keratinocytes as described previously [12]. Ax1W was used as the control vector to exclude the effect of Ax itself.

2.3. Real-time RT-PCR

Total RNA from cultured cells was isolated using Isogen (Nippon Gene, Japan). Real-time RT-PCR was performed and analyzed in an ABI PRISM 7700 sequence detector (Applied Biosystems, Branchburg, NJ). The primers and probes used for GAPDH, involucrin, and the PPARs were obtained from Applied Biosystems (Norwalk, CT). The RNA analysis was carried out using a TaqMan RT-PCR Master Mix Reagent Kit (Applied Biosystems). cDNA synthesis and PCR were performed and the level of gene expression was quantified using the comparative CT method as described previously [13]. The level of target gene expression in the test samples was

normalized against GAPDH and is reported as the difference relative to GAPDH.

2.4. Western blotting

Keratinocytes were harvested at specific times after treatment and whole cell lysates were extracted. Twenty micrograms of protein were separated by SDS-PAGE and transferred to polyvinylidene difluoride membranes. Analyses were performed using a Vistra ECF Kit (Amersham Biosciences, Arlington Heights, IL), and membranes were then scanned using a FluorolmageR (Molecular Dynamics, Sunnyvale, CA). The following antibodies were used for Western blotting: goat anti-β-actin (Santa Cruz Biotechnology, CA), rabbit anti-involucrin (Biomedical Technologies, Stoughton, MA), rabbit anti-Fra1 (Santa Cruz Biotechnology, CA), rabbit anti-c-Fos (Cell Signaling, Beverly, MA), rabbit anti-p38 and anti-phospho-p38 (Cell Signaling, Beverly, MA), and specific antibodies against PPARα, PPARβ/δ, PPARγ (Santa Cruz Biotechnology, CA) [6,14].

2.5. Preparation of nuclear extracts and electrophoretic mobility shift assays (EMSA)

Nuclear proteins were isolated, and the EMSA was performed as described previously [12] using a Light Shift® Chemiluminescent EMSA Kit (Pierce, Rockford, IL) according to the manufacturer's instructions. Specific PPARγ oligonucleotide probe sets (biotin-labeled and unlabeled probes) and AP-1 probe sets were obtained from Panomics (Redwood City, CA). For the supershift assays, nuclear extracts were preincubated with anti-Fra1 or anti-c-Fos antibody, or with species-matched control nonspecific IgG for 1 h at 4 °C, after which a biotin-labeled AP-1 probe was added. Protein–DNA complexes were separated and transferred to Biodyne® B nylon membranes (Pierce). The biotin-labeled molecules in the membranes were detected using a Chemiluminescent Nucleic Acid Detection Module (Pierce) and were exposed to X-ray film [12].

2.6. Luciferase assay

A reporter plasmid containing the involucrin promoter and firefly luciferase (pINV-Luc) was constructed as described previously [15]. To normalize the transfection efficiency, a plasmid containing *Renilla* luciferase driven by the herpes simplex virus thymidine kinase promoter (pRL-TK; Promega, Madison, WI) was included in the assay. The reporter plasmids were introduced into keratinocytes using FuGENE6 (Roche Molecular Biochemicals, Indianapolis, IN) according to the manufacturer's instructions. After treatment, the same number of cells was harvested with 250 μL of lysis buffer (Promega), and the luciferase activity was measured using the Dual-Luciferase Reporter Assay System (Promega) with a luminometer (Luminescencer JNR AB-2100; Atto, Japan). The relative luciferase activity was calculated by normalizing to the level of *Renilla* luciferase activity.

2.7. Chemicals

$1\alpha,25[OH]_2D_3$ was a generous gift from Teijin Pharmaceutical Co. Ltd. (Japan). In this study, 10^{-7} M $1\alpha,25[OH]_2D_3$ or same volume of EtOH (vehicle) was added into cultures. SB203580 was purchased from Calbiochem-Novabiochem International Co. (San Diego, CA) and dissolved in DMSO at 10 mM as a stock solution. One micromole SB203580 was added into cultures, and we did not detect cytotoxic effects in the keratinocytes treated with SB203580 using a cytotoxicity detection kit (Roche Diagnostics, German) (data not shown).

2.8. Statistical analysis

At least three independent experiments were performed, with similar results. One representative experiment is shown in each figure. The relative mRNA expression and relative luciferase activity are expressed as the mean ± S.D. ($n > 3$). Statistical significance was determined using Student's paired *t*-tests. Differences were considered statistically significant at $p < 0.05$ and indicated as $^*p < 0.05$ in the figures.

3. Results

3.1. Rapid induction and activation of PPARγ by $1\alpha,25(OH)_2D_3$

First, we investigated PPAR expression in $1\alpha,25(OH)_2D_3$-treated human keratinocytes. Real-time PCR analyses revealed that PPARα mRNA remained relatively constant over time with $1\alpha,25(OH)_2D_3$ treatment. Transcription of PPARβ/δ was increased slightly after stimulation for 48 h, whereas the expression of PPARγ was induced rapidly as early as 12 h after stimulation and was upregulated by more than 10-fold at 48 h (Fig. 1a). The expression of PPAR proteins was shown in Fig. 1b, PPARα, β/δ proteins were easily detected but remained unchanged during keratinocyte differentiation, confirmed the result from high calcium-induced differentiation [6]. Robust upregulation of

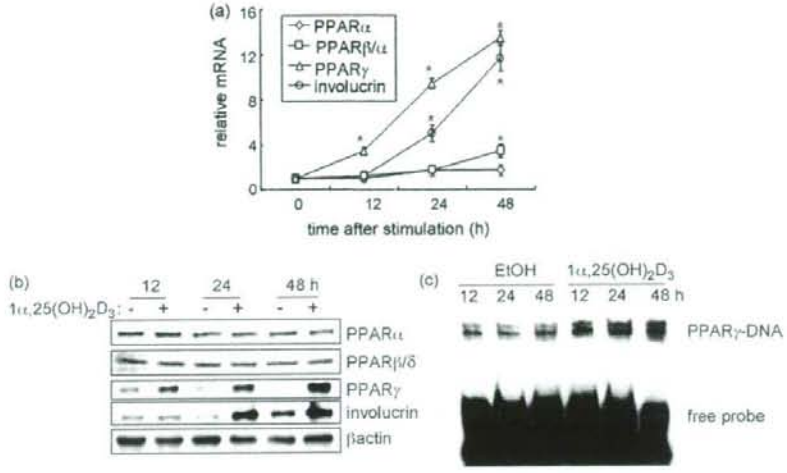

Fig. 1 $1\alpha,25(OH)_2D_3$ stimulates rapid induction and activation of PPARγ. (a) Subconfluent keratinocytes were incubated with $1\alpha,25(OH)_2D_3$ for the indicated times (0, 12, 24, 48 h). Total RNA was collected, and real-time RT-PCR was performed. (b) Keratinocytes were treated with $1\alpha,25(OH)_2D_3$ and collected after 12, 24, or 48 h of incubation. Total proteins were analyzed by Western blotting with antibodies against involucrin, PPARs, and β-actin. (c) Keratinocytes were exposed to $1\alpha,25(OH)_2D_3$, and nuclear extracts were collected at the indicated times (12, 24, or 48 h). A biotin-labeled PPARγ probe was incubated with the nuclear proteins, and EMSA was performed. The data are representative of at least three independent experiments.

PPARγ protein was observed in $1\alpha,25(OH)_2D_3$-treated keratinocytes, beginning at 12 h and peaking at 48 h (Fig. 1b). Next, we examined whether high expression of PPARγ results in specific signal activity in $1\alpha,25(OH)_2D_3$-induced keratinocyte differentiation. We performed EMSA to examine the DNA binding activity of PPARγ using nuclear keratinocyte extracts and a PPARγ-specific probe, which could not bind to PPARα or PPARβ protein [12]. The activity was up-regulated by $1\alpha,25(OH)_2D_3$, with a significant effect observed between 12 and 48 h post-treatment (Fig. 1c). According to a previous report [6], PPARγ protein is rarely detected in undifferentiated cells; however, we detected a substantial signal in vehicle cells using Western blotting (Fig. 1b) and EMSA (Fig. 1c). The conflicting results may be attributable to different culture conditions. For example, the keratinocytes used by Westeraard et al. [6] were isolated from adult skin, and the cells were collected when they reached 30–40% confluence. In our study, primary human keratinocytes from neonatal skin were stimulated at subconfluence. Moreover, the different culture media and experimental techniques may have also affected the results. Our data suggest that PPARγ is activated in differentiating keratinocytes induced by $1\alpha,25(OH)_2D_3$.

In $1\alpha,25(OH)_2D_3$-treated human keratinocytes, involucrin was induced after the expression and activation of PPARγ (Fig. 1a and b). This could suggest a causal relationship between PPARγ and involucrin expression in $1\alpha,25(OH)_2D_3$-treated human keratinocytes.

3.2. Regulation of $1\alpha,25(OH)_2D_3$-induced involucrin expression by PPARγ

Recent studies have shown that PPARγ ligands stimulate differentiation and promote involucrin expression directly or synergistically with PPARβ/δ ligand in both cultured human keratinocytes [6] and murine skin following topical application [7], implying that the PPARγ signal contributes to involucrin expression.

We hypothesized that activated PPARγ is important for $1\alpha,25(OH)_2D_3$-induced involucrin expression. No synthetic or natural PPARγ antagonists have been described as completely blocking PPARγ activation; therefore, to test our hypothesis, we constructed an adenovirus vector (Ax) carrying a dominant-negative mutant of PPARγ (Axdn-PPARγ) to inactivate the PPARγ signal [11]. To investigate the role of PPARγ in the activation of the involucrin promoter, we performed a luciferase assay. The $1\alpha,25(OH)_2D_3$-induced activity of the involucrin promoter was significantly inhibited by dn-PPARγ (Fig. 2a). Moreover, dn-PPARγ also suppressed the $1\alpha,25(OH)_2D_3$-induced expression of involucrin